

Temperature Dependence of Excitonic and Biexcitonic Decay Rates in Colloidal Nanoplatelets by Time-Gated Photon Correlation

Elad Benjamin,[†] Venkata Jayasurya Yallapragada,^{*,†} Daniel Amgar, Gaoling Yang, Ron Tenne, and Dan Oron^{*}Cite This: *J. Phys. Chem. Lett.* 2020, 11, 6513–6518

Read Online

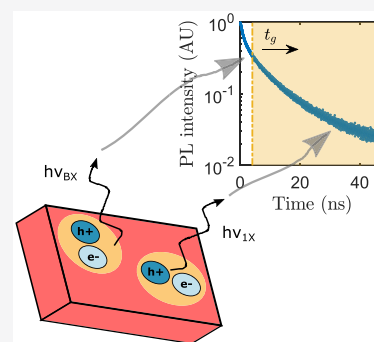
ACCESS |

Metrics & More

Article Recommendations

Supporting Information

ABSTRACT: Excitons in colloidal semiconductor nanoplatelets (NPLs) are weakly confined in the lateral dimensions. This results in significantly smaller Auger rates and, consequently, larger biexciton quantum yields, when compared to spherical quantum dots (QDs). Here we report a study of the temperature dependence of the biexciton Auger rate in individual CdSe/CdS core-shell NPLs, through the measurement of time-gated second-order photon correlations in the photoluminescence. We also utilize this method to directly estimate the single-exciton radiative rate. We find that whereas the radiative lifetime of NPLs increases with temperature, the Auger lifetime is almost temperature-independent. Our findings suggest that Auger recombination in NPLs is qualitatively similar to that of semiconductor quantum wells. Time-gated photon correlation measurements offer the unique ability to study multiphoton emission events, while excluding effects of competing fast processes, and can provide significant insight into the photophysics of a variety of nanocrystal multiphoton emitters.



Colloidal semiconductor nanocrystals (NCs) have been the subject of intense research during the past two decades. The nature of colloidal synthesis offers the possibility of tuning the optoelectronic properties of the NC by adjusting its size, composition, and geometry. Thus, NCs can potentially be used in many applications, e.g. LEDs, photovoltaic devices, biolabeling, and lasing media.^{1–5} In the past decade, flat, two-dimensional nanoplatelets (NPLs), with a thickness of a few atomic layers, have been synthesized. NPLs exhibit sharper absorption and emission peaks, a larger absorption cross section, directed emission, and a shorter radiative lifetime^{6–10} compared with their 0D (quantum dots) and 1D (nanorods) counterparts. These properties allow for promising lasing media, specifically as low gain threshold lasing media,^{5,11–13} and are determined in part by the dynamics of multiple excited (MX) states. In excited states involving three or more charge carriers, i.e. a charged exciton (trion), a biexciton (BX) or higher MX states, an additional nonradiative recombination path opens up, the Auger process, which is an important nonradiative recombination mechanism in NPLs.¹⁴ In Auger recombination an electron–hole pair recombines nonradiatively by exciting a third particle (electron or hole) to a higher energy level. The probability of such a process would increase if more excited carriers are present in close proximity to each other. In spherical quantum dots (QDs), because of the strong quantum confinement, the Auger rate is an order of magnitude higher than the radiative rate. In contrast, excitons in NPLs are weakly confined in the lateral dimensions, leading to a larger mean lateral separation between excitons. As a consequence, the Auger rate is an order of magnitude or more lower than in

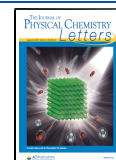
QDs or nanorods of the same volume, and the biexciton quantum yield (BXQY) is comparable to that of the single exciton (1XQY).^{9,15} Recent work done by Li et al. suggested that the Auger rate in NPLs scales inversely with the area of the NPL, unlike in QDs, where it scales inversely with the volume.¹⁶ While this work provided new understanding into the exciton dynamics in NPLs, it employed ensemble experimental approaches, such as time-resolved photoluminescence (PL) and transient absorption. These are sensitive to the effects of charging and photobleaching, as they rely on measurements at high excitation powers. Moreover, as with all ensemble measurements, their interpretation is challenging because of inhomogeneity within the probed ensemble, in properties such as absorption cross-section, recombination rates, and emitting state (e.g., excitons versus trions). Notably, both Li et al. and Amgar et al.¹⁷ show, using different methods (time-resolved spectroscopy and photon statistics, respectively), that the interaction between multiple excitons in NPLs, at least at room temperature, follows bimolecular interaction dynamics.

We use an alternative approach to probe multiexciton dynamics, based on the measurement of time-gated second-

Received: May 26, 2020

Accepted: July 22, 2020

Published: July 22, 2020



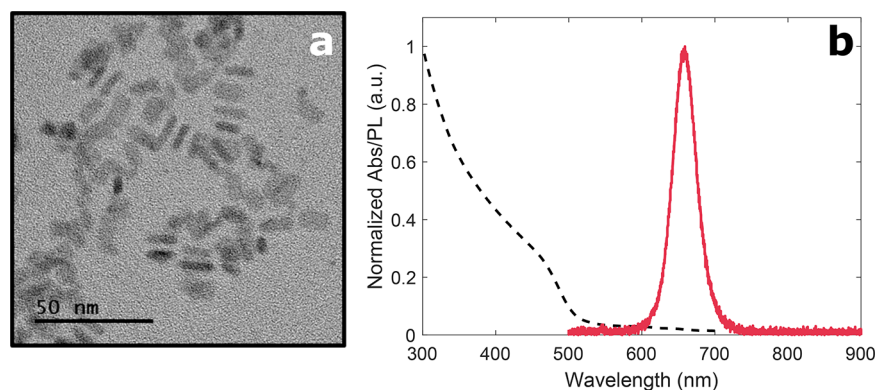


Figure 1. (a) TEM image of CdSe/CdS core/shell NPLs. (b) Absorption (dashed black line) and PL (solid red line) spectra of the same NPLs.

order photon correlations of the emitted PL from single NPLs.^{15,18,19} In such a measurement, light emitted from a single NPL is split onto two photon-counting detectors in a Hanbury-Brown and Twiss (HBT) type setup. In this configuration, the second-order temporal correlation function of the photon stream $g^{(2)}(\tau)$ is the probability of obtaining two detections, one in each detector, with a time difference τ between them. For a single-photon emitter, such as a single fluorescent molecule, it is theoretically impossible to record simultaneous photon arrival events in both detection arms and $g^{(2)}(0) = 0$. This phenomenon is called *photon antibunching* and is often used to test whether an emitter is a single-photon emitter.²⁰

In single, core-only or core/thin-shell QDs, the BXQY is typically much lower than the 1XQY; therefore, the chance to detect a photon pair at delay $\tau = 0$ is small, and this leads to a small value of $g^{(2)}(0)$. However, NPLs exhibit a higher BXQY, which results in values of $g^{(2)}(0)$ well above zero. The ratio between the BXQY and the 1XQY can be determined from the statistics of detected photon pairs.²¹ These statistics are directly connected to the recombination dynamics of the BX, because BX emission always precedes 1X emission. Thus, combining measurements of $g^{(2)}(0)$ with selection of photon detections according to their arrival times provide us a route to extracting the rate of Auger recombination, which limits the BXQY in NPLs.¹⁹ Also, notably, in this *time-gated* $g^{(2)}(\tau)$, the measured value of the Auger rate is indifferent to the existence of single-exciton nonradiative pathways and therefore is significantly less sensitive to the intermittent nature of PL in colloidal nanocrystals (NC blinking).

Here we use the analysis of time-gated photon statistics to study the temperature dependence of both the single-exciton radiative rate and the biexciton Auger rate in CdSe/CdS core/shell NPLs, where the emission is known to exhibit multiexponential decay dynamics even at low excitation fluences.^{7,9,22}

CdSe/CdS core/shell NPLs were synthesized following literature methods.^{23,24} Cores are composed of 5 monolayer CdSe NPLs for which the lowest energy exciton absorption peak (electron-heavy hole) and the PL peak were measured at 542 and 547 nm, respectively. The average lateral dimensions of the cores are 5.2 ± 0.9 nm \times 12 ± 1 nm as measured by TEM. Those were subsequently passivated by 3 monolayers of CdS shell, leading to a red shift of the emission peak to 659 nm. A TEM image of the NPLs as well as their absorption and emission spectra are given in Figure 1. Full details of the

synthesis and characterization methods can be found in Amgar et al.¹⁷

Our measurement setup is based on a fluorescence confocal microscope built around an optical cryostat. The sample is prepared by drop casting a dilute suspension of NPLs on a silicon wafer (380 μ m Si + 100 nm SiO₂, MicroChemicals GmbH). The dilution is made so that particles are sparse enough to prevent two NPLs clustered within a diffraction-limited spot of the excitation beam. The sample is mounted inside the optical cryostat (Montana instruments cryostation) used to set the sample temperature within the range of 4.5 K to room temperature. We excite a single NPL using a super-continuum source (Fianium Whitelase) producing 100 ps pulses centered at 470 nm with a repetition rate of 20 MHz, operated at an average power of 10 μ W. The excitation pulse is focused onto a diffraction-limited spot on the sample by an excitation objective (Zeiss EC Plan-NEOFLUAR, NA 0.5). Light emitted from the NPL is then collected by the same objective, spectrally filtered, and coupled into a multimode optical fiber-based 50/50 beam splitter. It is then detected with two SPADs (Excelitas technologies SPCM AQ4C) connected to a time-correlated single-photon-counting (TCSPC) module (Picoquant Hydraharp 400) operated in a time-tagged mode. This enables us to perform photon correlation analysis in post processing, also with respect to the arrival time of the excitation pulse. Cooled particles were measured at temperatures varying from 4 to 150 K, above which the NPLs became too dim to measure effectively. This behavior was previously demonstrated and attributed to the effect of the vacuum in the cryostat on the trapping/detrapping of surface states.⁷ Room-temperature measurements were carried out with the cryostat vented.

We define the second-order photon correlation function as

$$g^{(2)}(\tau) = \frac{G^{(2)}(\tau)}{G^{(2)}(\tau \rightarrow \infty)} \quad (1)$$

where $G^{(2)}(\tau)$ is the number of photon pairs emitted with a time difference τ between them and $G^{(2)}(\tau \rightarrow \infty)$ is the number of photon pairs emitted at an arbitrarily large delay (chosen here to be any delay longer than the laser period, which is much longer than the characteristic decay dynamics of the NPLs). Taking the τ resolution to be the repetition rate (meaning photons arriving following the same pulse are considered as coincident), for zero delay ($\tau = 0$) the numerator would be the result of photon pairs emanating from biexciton recombination, while the denominator mostly includes

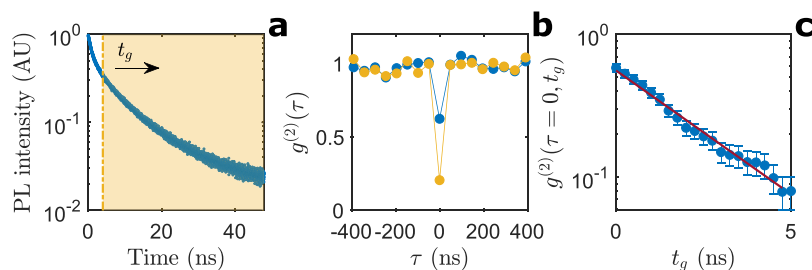


Figure 2. Representative measurement of a single NPL. (a) Decay of PL intensity in time. Photons corresponding to arrival times greater than t_g (inside the yellow shaded area) are used to generate $g^{(2)}(\tau)$. t_g is scanned in the arrow's direction, excluding more photons for greater t_g . (b) Second-order correlation functions for two choices of t_g , 0 in blue and 4 ns in yellow. (c) $g^{(2)}(0)$ as a function of t_g in blue circles. The solid red line is a fit to a single-exponential function. $\tau_A = 2.5$ ns with $R^2 = 0.98$. Error bars are the deviation in the number of pairs at delay 0, according to Poisson distribution.

photons from single-exciton recombination at different pulses. The previous statement is conditioned on non-saturating excitation of the NPL, so that the probability of exciting highly excited states (more than two excitations per pulse) is negligible. BX emission is a cascaded process; the NC decays from the BX state to the 1X state while emitting a photon, followed by a recombination of the 1X state and emission of a second photon. Therefore, photons emitted at long delays after the exciting pulse are more likely to result from the recombination of the 1X state. To take advantage of this, we exclude from our analysis all photons that were emitted before a specific time after each pulse, which we term the *gating time* (t_g). We then calculate $g^{(2)}(\tau)$ for this subset of all detected photons. By doing that we exclude a higher proportion of the first photons of BX emission cascades, which in turn would result in fewer coincidence detections and so a decrease in $g^{(2)}(\tau = 0)$. The exact magnitude of the decrease in $g^{(2)}(0)$ for a given gating time depends on both the 1X and BX lifetimes. Performing the calculation of $g^{(2)}(\tau = 0)$ with respect to a specific t_g explicitly, we arrive at (the full derivation, as well as the estimation of background contribution to $g^{(2)}(\tau = 0, t_g)$ can be found in Sections S1 and S2 of the Supporting Information; also see Magnum et al.¹⁹)

$$g^{(2)}(\tau = 0, t_g) = \frac{2k_{1X}}{2k_{1X} + k_A} e^{-k_A t_g} \quad (2)$$

where t_g is the gating time and k_A is the Auger rate. k_{1X} is the single-exciton recombination rate, taking into account both radiative and nonradiative processes. We assume here that the biexciton dynamics follows bimolecular recombination kinetics; that is, the non-Auger biexciton recombination rate is double that of the exciton.^{16,17} Clearly, with these assumptions, the decay of $g^{(2)}(0, t_g)$ with the gating time is exponential and actually depends only on the Auger rate. NPLs, like other types of NCs, exhibit intermittency (“on” and “off” periods) in photoluminescence, termed *blinking*. The “on” and “off” periods are characterized by different radiative lifetimes, often because of the presence of various nonradiative mechanisms. The form of eq 2 implies that the time gating process decouples the Auger mechanism from other non-radiative pathways. Therefore, with the exception of trion emission, this method of measuring the Auger lifetime is significantly less sensitive to NPL blinking. Emission from trion states could skew both the amplitude and exponent of $g^{(2)}(0, t_g)$, as it involves 3 charge carriers and can also nonradiatively recombine via the Auger pathway. However, because in NPLs the Auger rate is slower than in quantum dots, it is likely that

charging would not dramatically change the time-gated correlation function. Notably, at zero gating time, where we do not discard any photons, we get the known result:²¹

$$g^{(2)}(\tau = 0) = \frac{2k_{1X}}{2k_{1X} + k_A} = \frac{BXQY}{1XQY} \quad (3)$$

In the following analysis, the Auger rate is obtained for each NPL by fitting the data to eq 2.

Our method of performing the “time-gated $g^{(2)}$ ” measurement and analysis is demonstrated in Figure 2. When the full set of data shown in the decay curve in Figure 2a is used, the blue $g^{(2)}$ curve of Figure 2b is obtained, and using a gating time of 4 ns (yellow shaded area in Figure 2a), we get the yellow curve. The blinking trace associated with this specific measurement is given in Figure 3a. Further details of the correlation measurement, as well as a high temporal resolution of Figure 2b, are given in Figure S1. As can be seen in Figure 2c, the value of $g^{(2)}(0)$ decreases with t_g as expected and in fact

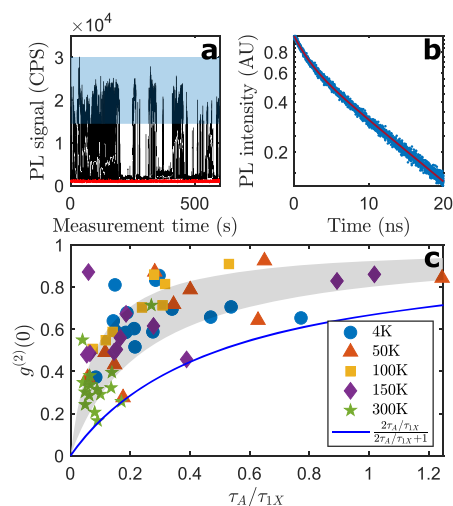


Figure 3. (a) PL as a function of measurement time of a representative single NPL, solid black line. NPL exhibits “blinking”, the “on” state is in the blue shaded area. Background signal is in solid red. (b) PL decay transient extracted only from the “on” state (blue dots). Fit to a biexponential function is in solid red, $\tau_{1X} = 11.1$ ns. (c) $g^{(2)}(0)$ without gating as a function of τ_A/τ_{1X} of several NPLs at 4 K (blue circles), 50 K (red triangles), 100 K (yellow squares), 150 K (purple diamonds), and 300 K (green stars). The dependence predicted by the model, as expressed in eq 4 is shown in solid blue. Shaded in gray are prediction curves with τ_A/τ_{1X} smaller by a factor between 2 and 6.

goes below the value of 0.5, indicating the measured NPL is indeed a single particle. $g^{(2)}(0, t_g)$ is well fitted by a decreasing single-exponential function, from which the measured Auger lifetime (inverse of the Auger rate) is extracted: $\tau_A = 1/k_A = 2.5$ ns. We repeat this procedure at several temperatures between 4 and 300 K and for multiple particles at each temperature. The single-exponential nature of the dependence of the measured $g^{(2)}(0, t_g)$ on t_g indicates that our underlying assumptions are likely satisfied, i.e., correlations emanating from higher excited states do not play a significant role in the observed dynamics. A measurement of PL intensity as a function of excitation power is given in Figure S2, and an estimation of the average number of photons absorbed per pulse is indeed much smaller than 1 (of the order of 0.1) as given in Section S3 in the Supporting Information.

We note that eq 2 can be rewritten for $t_g = 0$ as a function of the form

$$g^{(2)}(0, x) = \frac{2x}{2x + 1} \quad (4)$$

where $x = \frac{k_{1X}}{k_A} = \frac{\tau_A}{\tau_{1X}}$. This implies that if our model indeed accurately describes the recombination dynamics of excitons in the NPLs, while the Auger and radiative lifetimes may have a different dependence on temperature, the value of $g^{(2)}(\tau = 0, t_g = 0)$ as a function of their ratio should fall on the line described by eq 4. To test this we have to provide an independent estimate of the 1X radiative lifetime. This can be done by fitting the PL decay to a multiexponential function. To exclude variations of the emission decay due to blinking, we isolate the “on” state decay statistics of each single NPL and fit them to a biexponential decay function. We attribute the slower of the two decay components in this biexponential fit to the 1X decay (see Figure 3a,b). A scatter plot of $g^{(2)}(0)$ versus τ_A/τ_{1X} at various temperatures is shown in Figure 3c, where we post-selected only isolated single particles whose $g^{(2)}(0, t_g)$ fell below 0.25 at long t_g , and who showed pure single-exponential behavior in the gated $g^{(2)}(0)$ measurement described in Figure 2c.

Looking at Figure 3c, it is clear that indeed all NPLs measured at all temperatures seem to follow a universal trend regardless of the specific value of $g^{(2)}(0)$ for the particular NPL, indicating that $g^{(2)}(0)$ indeed depends only on the ratio of the two extracted quantities: the radiative lifetime and the Auger lifetime. Notably, while in cryo temperatures the spread in both x and y values is quite wide, the data points for 300 K cluster around the bottom left part of the graph. This is a consequence of an appreciable increase in the radiative lifetime while the Auger lifetime remains nearly constant (see Figure 4 and subsequent discussion). However, the measured $g^{(2)}(0)$ values seem to be consistently above the prediction of eq 4. This deviation could be remedied if the 1X radiative lifetimes were shorter by a factor of 2–6 (approximately 3.5 on average, see Figure 4b) than the ones we estimate from the slowest arriving photons, represented in Figure 3c by the gray shaded area overlapping the majority of data points. A possible explanation for this discrepancy is a mechanism for carrier trapping and detrapping, leading to delayed emission, a significant effect in quantum dot exciton dynamics.^{25,26} For the case of CdSe/CdS core/shell NPLs, Rabouw et al. estimate that delayed emission accounts for approximately 16% of the emitted photons and in fact dominates the emission at time scales larger than 20 ns.²⁷ In such a case, the observed decay

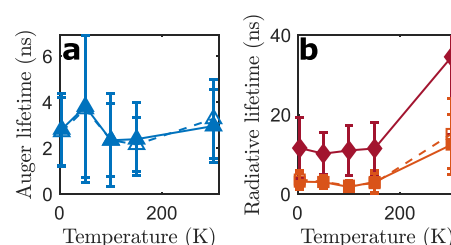


Figure 4. (a) Mean values of BX Auger lifetimes with (dashed blue triangles) and without (solid blue triangles) PL intensity selection, at different temperatures. (b) Mean values of single-exciton radiative lifetime with (dashed red squares) and without (solid red squares) PL intensity selection, at different temperatures. Solid dark-red diamonds represent the mean radiative lifetime estimated from the slow component of the on state. Error bars present the standard deviation of each ensemble average.

rate would extend beyond the radiative lifetime, and a fit to a biexponential function would overestimate the radiative lifetime because of the inclusion of delayed emission in the fit. In fact, this measurement provides us with an alternative, self-consistent estimate of the radiative lifetime as a function of temperature.

Figure 4 shows the mean Auger lifetime measured from the gated photon statistics versus temperature (a), as well as the mean single-exciton radiative lifetime versus temperature as estimated both from the amplitude of $g^{(2)}(0)$ and from the fit to the biexponential decay (b). We observe that the radiative lifetime appears to slowly increase with temperature for low temperatures and then more rapidly increases at a temperature range above 150 K. This is consistent with the findings of previous studies.^{6,7} The lifetimes estimated from the fit to the biexponential decay and those obtained from the amplitude of the correlation function exhibit a qualitatively similar variation with temperature but are roughly 3.5 times longer, as is evident from Figure 3c. On the other hand, within our experimental uncertainty the Auger lifetime exhibits little to no dependence on temperature. This is in agreement with the theoretical predictions for QWs. For wells with small well widths (≤ 50 Å), the theoretical calculations yield an Auger rate which is nearly independent of the temperature.²⁸

To directly demonstrate the insensitivity of this method to NPL blinking, the aforementioned lifetimes are compared to the results obtained after applying PL intensity selection, in the same manner as in Figure 3a, before calculating the time-gated correlation function. As expected, the results obtained with and without intensity selection are nearly identical.

In summary, we utilized time-gated second-order photon correlation to estimate the Auger recombination rate of the biexciton state in individual colloidal NPLs. By suitably postselecting photon detection events to include only photons that are detected after a gating time t_g , we were able to determine the Auger rate directly from the dependence of the correlation function $g^{(2)}(0)$ on t_g . Inspection of the functional form of $g^{(2)}(0)$ with respect to the ratio between the Auger and the single-exciton radiative lifetimes ($\frac{\tau_A}{\tau_{1X}}$) at different temperatures indicates that this method can provide an alternative, self-consistent estimate of the radiative lifetime even for NCs exhibiting a multiexponential decay behavior. Applying this method on individual colloidal core/shell CdSe/CdS NPLs maintained at various temperatures, we have shown that there is no significant change in the Auger rate between 4 and 150 K

and up to room temperature. This supports the hypothesis that nonradiative recombination in NPLs is more similar to QWs than to QDs. As the method used here is based on heuristic principles and independent of physical considerations imposed by the materials constituting the particles and their geometry, it may be generally applicable to many 1D and 2D materials, providing a new tool in the study of MX dynamics in NCs with a nonzero BXQY.

■ ASSOCIATED CONTENT

SI Supporting Information

The Supporting Information is available free of charge at <https://pubs.acs.org/doi/10.1021/acs.jpcllett.0c01628>.

High-resolution $g^{(2)}(\tau)$, PL intensity versus excitation power, spectra of a single NPL, derivation of $g^{(2)}(0)$ as a function of the gating time, estimation of the background contribution to $G^{(2)}(\tau = 0, t_g)$, and estimation of the average number of photons absorbed per pulse (PDF)

■ AUTHOR INFORMATION

Corresponding Authors

Venkata Jayasurya Yallapragada – Department of Physics of Complex Systems, Weizmann Institute of Science, Rehovot 76100, Israel; orcid.org/0000-0001-9129-6414; Email: venkata-jayasurya.yallapragada@weizmann.ac.il

Dan Oron – Department of Physics of Complex Systems, Weizmann Institute of Science, Rehovot 76100, Israel; orcid.org/0000-0003-1582-8532; Email: dan.oron@weizmann.ac.il

Authors

Elad Benjamin – Department of Physics of Complex Systems, Weizmann Institute of Science, Rehovot 76100, Israel; orcid.org/0000-0002-5980-7103

Daniel Amgar – Department of Physics of Complex Systems, Weizmann Institute of Science, Rehovot 76100, Israel; orcid.org/0000-0001-8379-187X

Gaoling Yang – Department of Physics of Complex Systems, Weizmann Institute of Science, Rehovot 76100, Israel; orcid.org/0000-0003-2218-1781

Ron Tenne – Department of Physics of Complex Systems, Weizmann Institute of Science, Rehovot 76100, Israel

Complete contact information is available at:

<https://pubs.acs.org/doi/10.1021/acs.jpcllett.0c01628>

Author Contributions

[†]E.B. and V.J.Y. contributed equally to this work.

Notes

The authors declare no competing financial interest.

■ ACKNOWLEDGMENTS

This work was supported by ERC Consolidator grant ColloQuantO and by the Crown Center of Photonics. D.O. is the incumbent of the Harry Weinrebe chair in laser physics.

■ REFERENCES

(1) Talapin, D. V.; Lee, J.-S.; Kovalenko, M. V.; Shevchenko, E. V. Prospects of Colloidal Nanocrystals for Electronic and Optoelectronic Applications. *Chem. Rev.* **2010**, *110*, 389–458.

(2) Kubacka, A.; Fernández-García, M.; Colón, G. Advanced Nanoarchitectures for Solar Photocatalytic Applications. *Chem. Rev.* **2012**, *112*, 1555–1614.

(3) Michalet, X. Quantum Dots for Live Cells, in Vivo Imaging, and Diagnostics. *Science* **2005**, *307*, 538–544.

(4) Kazes, M.; Lewis, D. Y.; Ebenstein, Y.; Mokari, T.; Banin, U. Lasing from Semiconductor Quantum Rods in a Cylindrical Microcavity. *Adv. Mater.* **2002**, *14*, 317–321.

(5) She, C.; Fedin, I.; Dolzhenkov, D. S.; Demortière, A.; Schaller, R. D.; Pelton, M.; Talapin, D. V. Low-Threshold Stimulated Emission Using Colloidal Quantum Wells. *Nano Lett.* **2014**, *14*, 2772–2777.

(6) Ithurria, S.; Tessier, M. D.; Mahler, B.; Lobo, R. P. S. M.; Dubertret, B.; Efron, A. L. Colloidal nanoplatelets with two-dimensional electronic structure. *Nat. Mater.* **2011**, *10*, 936–941.

(7) Tessier, M. D.; Javaux, C.; Maksimovic, I.; Lorient, V.; Dubertret, B. Spectroscopy of Single CdSe Nanoplatelets. *ACS Nano* **2012**, *6*, 6751–6758.

(8) Achtstein, A. W.; Schliwa, A.; Prudnikau, A.; Hardzei, M.; Artemyev, M. V.; Thomsen, C.; Woggon, U. Electronic Structure and Exciton-Phonon Interaction in Two-Dimensional Colloidal CdSe Nanosheets. *Nano Lett.* **2012**, *12*, 3151–3157.

(9) Kunneman, L. T.; Tessier, M. D.; Heuclin, H.; Dubertret, B.; Aulin, Y. V.; Grozema, F. C.; Schins, J. M.; Siebbeles, L. D. A. Bimolecular Auger Recombination of Electron–Hole Pairs in Two-Dimensional CdSe and CdSe/CdZnS Core/Shell Nanoplatelets. *J. Phys. Chem. Lett.* **2013**, *4*, 3574–3578.

(10) Gao, Y.; Weidman, M. C.; Tisdale, W. A. CdSe Nanoplatelet Films with Controlled Orientation of their Transition Dipole Moment. *Nano Lett.* **2017**, *17*, 3837–3843.

(11) She, C.; Fedin, I.; Dolzhenkov, D. S.; Dahlberg, P. D.; Engel, G. S.; Schaller, R. D.; Talapin, D. V. Red, Yellow, Green, and Blue Amplified Spontaneous Emission and Lasing Using Colloidal CdSe Nanoplatelets. *ACS Nano* **2015**, *9*, 9475–9485.

(12) Li, Q.; Xu, Z.; McBride, J. R.; Lian, T. Low Threshold Multiexciton Optical Gain in Colloidal CdSe/CdTe Core/Crown Type-II Nanoplatelet Heterostructures. *ACS Nano* **2017**, *11*, 2545–2553.

(13) Li, Q.; Liu, Q.; Schaller, R. D.; Lian, T. Reducing the Optical Gain Threshold in Two-Dimensional CdSe Nanoplatelets by the Giant Oscillator Strength Transition Effect. *J. Phys. Chem. Lett.* **2019**, *10*, 1624–1632.

(14) Baghani, E.; O’Leary, S. K.; Fedin, I.; Talapin, D. V.; Pelton, M. Auger-Limited Carrier Recombination and Relaxation in CdSe Colloidal Quantum Wells. *J. Phys. Chem. Lett.* **2015**, *6*, 1032–1036.

(15) Ma, X.; Diroll, B. T.; Cho, W.; Fedin, I.; Schaller, R. D.; Talapin, D. V.; Gray, S. K.; Wiederrecht, G. P.; Gosztola, D. J. Size-Dependent Biexciton Quantum Yields and Carrier Dynamics of Quasi-Two-Dimensional Core/Shell Nanoplatelets. *ACS Nano* **2017**, *11*, 9119–9127.

(16) Li, Q.; Lian, T. Area- and Thickness-Dependent Biexciton Auger Recombination in Colloidal CdSe Nanoplatelets: Breaking the “Universal Volume Scaling Law. *Nano Lett.* **2017**, *17*, 3152–3158.

(17) Amgar, D.; Yang, G.; Tenne, R.; Oron, D. Higher-Order Photon Correlation as a Tool To Study Exciton Dynamics in Quasi-2D Nanoplatelets. *Nano Lett.* **2019**, *19*, 8741–8748.

(18) Deutsch, Z.; Schwartz, O.; Tenne, R.; Popovitz-Biro, R.; Oron, D. Two-Color Antibunching from Band-Gap Engineered Colloidal Semiconductor Nanocrystals. *Nano Lett.* **2012**, *12*, 2948–2952.

(19) Mangum, B. D.; Ghosh, Y.; Hollingsworth, J. A.; Htoon, H. Disentangling the effects of clustering and multi-exciton emission in second-order photon correlation experiments. *Opt. Express* **2013**, *21*, 7419.

(20) Gerry, C.; Knight, P. *Introductory Quantum Optics*; Cambridge University Press, 2004.

(21) Nair, G.; Zhao, J.; Bawendi, M. G. Biexciton Quantum Yield of Single Semiconductor Nanocrystals from Photon Statistics. *Nano Lett.* **2011**, *11*, 1136–1140.

(22) Tessier, M. D.; Mahler, B.; Nadal, B.; Heuclin, H.; Pedetti, S.; Dubertret, B. Spectroscopy of Colloidal Semiconductor Core/Shell

Nanoplatelets with High Quantum Yield. *Nano Lett.* **2013**, *13*, 3321–3328.

(23) Tessier, M. D.; Spinicelli, P.; Dupont, D.; Patriarche, G.; Ithurria, S.; Dubertret, B. Efficient Exciton Concentrators Built from Colloidal Core/Crown CdSe/CdS Semiconductor Nanoplatelets. *Nano Lett.* **2014**, *14*, 207–213.

(24) Yang, Z.; Pelton, M.; Fedin, I.; Talapin, D. V.; Waks, E. A room temperature continuous-wave nanolaser using colloidal quantum wells. *Nat. Commun.* **2017**, *8*, 143.

(25) Rabouw, F. T.; Kamp, M.; van Dijk-Moes, R. J. A.; Gamelin, D. R.; Koenderink, A. F.; Meijerink, A.; Vanmaekelbergh, D. Delayed Exciton Emission and Its Relation to Blinking in CdSe Quantum Dots. *Nano Lett.* **2015**, *15*, 7718–7725.

(26) Mondal, N.; Naphade, R.; Zhou, X.; Zheng, Y.; Lee, K.; Gereige, I.; Al-Saggaf, A.; Bakr, O. M.; Mohammed, O. F.; Gartstein, Y. N.; et al. Dynamical Interconversion between Excitons and Geminate Charge Pairs in Two-Dimensional Perovskite Layers Described by the Onsager-Braun Model. *J. Phys. Chem. Lett.* **2020**, *11*, 1112–1119.

(27) Rabouw, F. T.; van der Bok, J. C.; Spinicelli, P.; Mahler, B.; Nasilowski, M.; Pedetti, S.; Dubertret, B.; Vanmaekelbergh, D. Temporary Charge Carrier Separation Dominates the Photoluminescence Decay Dynamics of Colloidal CdSe Nanoplatelets. *Nano Lett.* **2016**, *16*, 2047–2053.

(28) Polkovnikov, A. S.; Zegrya, G. G. Auger recombination in semiconductor quantum wells. *Phys. Rev. B: Condens. Matter Mater. Phys.* **1998**, *58*, 4039–4056.